Int. J. Electrochem. Sci., 11 **(2016)** 4794 – 4801, doi: 10.20964/2016.06.4

International Journal of
ELECTROCHEMICAL
SCIENCE
www.electrochemsci.org

Short Communication

Reduced Graphene Oxide Encapsulated N-type Si Nanoparticles as Anode for Lithium-ion Batteries

Zhongwei Luo, Taotao Ding, Jiangnai Dai[*], *Changqing Chen*[*]

Wuhan National Laboratory for Optoelectronics, Huazhong University of Science and Technology, Wuhan 430074, China.
[*]E-mail: cqchen@hust.edu.cn, daijiangnan@hust.edu.cn

Received: 16 February 2016 / *Accepted:* 22 March 2016 / *Published:* 4 May 2016

Silicon is generally considered as the next generation of anode materials for lithium-ion batteries because of its highest theoretical specific capacity of all the known materials. However its low initial coulombic efficiency, poor cyclic performance and expensive silicon nanoparticles limit its application for anode. Here, we report a simple and inexpensive synthetic method of RGO/n-Si composite in which n-Si nanoparticles were encapsulate by thermal reduced graphene oxide, in which the thermal reduced garphene oxide buffers the huge volume changes of Si during lithiation and delithiation. Besides, Si nanoparticles doped with P can improve the electrical conductivity of anode. As a result, these graphene encapsulated n-type Si nanoparticles have a much improved cyclic stability with a reversible capacity of 1529 mAh/g over 200 cycles.

Keywords: Si; n-Si, graphene, lithium-ion batteries.

1. INTRODUCTION

Since rechargeable lithium ion batteries (LIBS) were invented by Sony in 1990, they were used in many fields, which is due to their many advantages, such as lighter weight, higher energy density, longer cycle life,more environmentally friendly than the traditional lead-acid batteries, etc[1]. However commercial lithium ion batteries anode materials are still using graphite as anode, which hadn't changed too much for nearly twenty years. Inaddition, they were suffering from low specific capacity[2]. Hence, researches for high capacity lithium ion battery anode materials have become the key to improve the battery storage performance[3]. Various anode materials have been studied in terms of high storage capacity and cyclic stability in the last couple of decades[4]. Among these, silicon is considered to be the next generation lithium-ion anode materials with the highest theoretical specific

capacity ($Li_{4.4}Si$=4200 mAh/g) of all the known materials and mature silicon semiconductor industry[5-7].

However, the application of silicon still have significant challenges such as large volume changes (＞300%) during lithiation and delithiation, unstable solid-electrolyte interphases (SEI), low electrical conductivity and low coulombic efficiency[8-10]. The large volume expansion will cause severe particle fracture, the continuous loss of electrical contact with the copper foil, and rapid capacity attenuation. Many efforts have been made to overcome these problems. Among these, constructing nanostructure electrode, such as silicon nanospheres[11], silicon nanowires [8,12], and silicon nanotubes[13-15] are the most effective strategies, for these nanostructures，which are much easier to adjust to the huge volume change than bulk Si during Li+ insertion and extraction.

Nevertheless, expensive and inefficient processes are inevitable used in the synthetic of these Si-based anodes. For example, Holzapfel synthesized silicon/graphite compound material received a reversible capacity of 1900 mAh/g for over 100 cycles by chemical vapor deposition (CVD)[16]. Jung reported an amorphous silicon thin film which exhibited a high reversible capacity of 4000 mAh/g by low pressure CVD[17].

Alternative strategy is to fabricate Si/C nanostructure composites. Cui reported a carbon-silicon core-shell with a high charge storage capacity of 2000 mAh/g[18]. Lee reported the Silicon nanoparticles–graphene paper composites with a storage capacity 1500 mAh/g for 200 cycles[19]. And the graphene/Si composites with high capacities and good cyclic stability were prepared by Fu et al[20,21].

As the first generation of semiconductor, the intrinsic conductivity of silicon is only $6.7x10^{-4}$ S/cm at room temperature. However, there were few reports about improving the electrical conductivity of silicon. Herein we reported an effective way to synthesis P-doped silicon nanoparticles (n-Si) coated with thermal reduced graphene(RGO/n-Si). In which, the graphene work as an elastic skeleton can envelop the Si nanoparticles for preventing exposing to electrolyte, buffering the deformation stresses and Si nanoparticles doping with P can improve the low electrical conductivity. The RGO/n-Si nanoparticles show a high reversible lithium-storage capacity (1529 mAh/g), prominent cyclic performance, and good rate charge-discharge capability.

2. EXPERIMENTAL

2.1. Materials synthesis

2.1.1. Synthesis of n-type Si nanoparticles

The P doped Si nanoparticles with an average particle size of 16 nm were produced by a plasma system. The SiH_4 and dopant precursor trimethyl phosphite (TMP) were carried into the plasma system by Ar at the rate of 1:9. The flow rate of TMP, SiH_4 and Ar was 100, 100, 500 (sccm), respectively. The power of the plasma system was set to 450 W to excite plasma and maintain stable homogeneous glow discharge.

2.1.2. Synthesis of garphene oxide

Graphene oxide (GO) was synthesized from natural flake graphite by a modified Hummers method[22]. The natural flake graphite(0.6 g) was mixed with $KMnO_4$ (3.6 g), and then add H_3PO_4 and H_2SO_4 mixed solution to the above mixture to heat in water bath at 50℃ for 12 h. After that, ice (80g) was added to the above mixed solution. The suspension was washed with 5% HCl solution after the color was changed from violet to golden yellow when adding 3ml H_2O_2. It was then centrifuged(8000 rpm, 60 min) 7~10 times with deionized water for 2 days until the PH is nearly 7. Finally, the GO sheets were obtained by dehydration at 60 °C in air.

2.1.3. Preparation of RGO/Si composite

The RGO/n-Si composite was synthesized by a simple method. Typically, the GO solution (2 mg/mL) and n-type Si nanoparticles alcohol suspension (6 mg/mL) were ultrasonic dispersed for 90 min and 30 min, respectively. It was then magnetic stirred for 4 h with a mixture of GO solution and Si nanoparticles alcohol at the volume ratio of 1:1 (50 mL: 50 mL). After that, the GO encapsulated n-Si (GO/n-Si) composite was formed by suction filtration and vacuum dried at 60℃ for 12 h. Finally, the GO/n-Si was annealed at 700℃ for 1 h with a heating rate of 10℃/min under the Ar atmosphere (100 sccm) to obtain the RGO coated n-Si composite.

2.2. Characterization of Si/graphene composites

Powder X-ray diffraction (XRD) analysis was performed on a Bruker D8 Advance X-ray diffractometer with Cu Ka radiation (XRD, λ= 1.5418 Å). The scattering angles (2θ) were from 10 º to 80 º, and the scanning rate was 10 º per minute. Scanning electron microscopy (SEM) was carried out using a LEO 1530 VP field emission scanning electron microscope with an acceleration voltage of 10 kV. Transmission electron microscopy (TEM) was performed on a Tecnai G2 F30 (FEI, Holland) transmission electron microscope operated at 200 kV.

2.3. Battery assembly and electrochemical characterization

The working electrode was prepared with RGO/n-Si composite, Super P carbon black and sodium carboxymethylcellulose (CMC) mixed at the mass ratio of 8 : 1 : 1. Deionized water was added to the homogeneous powdered mixture to obtain a viscous slurry. The electrode sheet was obtained after magnetic stirring for 12 h and coated onto a 9 μm Cu foil followed with vacuum drying at 60℃ for 12 h. 10 mm diameter electrodes with a mass loading of 1.0 mg were obtained via punching on the surface of the electrode sheet after which was pressed. The coin-type cells (CR2025) were assembled in an Ar-filled glove box with moisture and oxygen concentrations strictly controlled below 1 ppm. Lithium metal foil was used as the counter electrode, and 1 M $LiPF_6$ dissolved in ethylene carbonate/diethyl carbonate (EC:DEC=1:1, v/v) as the electrolyte. The charge/discharge measurements

were performed by using LAND CT2001A battery test system (Wuhan LAND Electronics. Ltd.) with potential (*vs*. Li^+/Li) between 0.01 v and 1.5 v at room temperature.

3. RESULTS AND DISCUSSION

Figure 1 shows a schematic of the fabrication of the RGO/n-Si composite. Firstly, n-Si nanoparticles and GO were prepared by a plasma system and a modified Hummers method， respectively. And then n-Si nanoparticles and GO solution were mixed by magnetic stirring to acquire a homogeneous GO/n-Si solution. Secondly, the GO/n-Si solution was filtered and vacuum dried at 60 ℃ for 12 h. Finally, through a thermal annealing treatment at Ar atmosphere for 1 h, the RGO/n-Si composite was obtained. The RGO has an elastic and robust structure which can buffer the large volume changes in the electrochemical reactions of silicon electrodes. In order to improve the low electrical conductivity of Si nanoparticles, TMP was carried into a plasma system as dopant precursor to dope silicon nanoparticles.

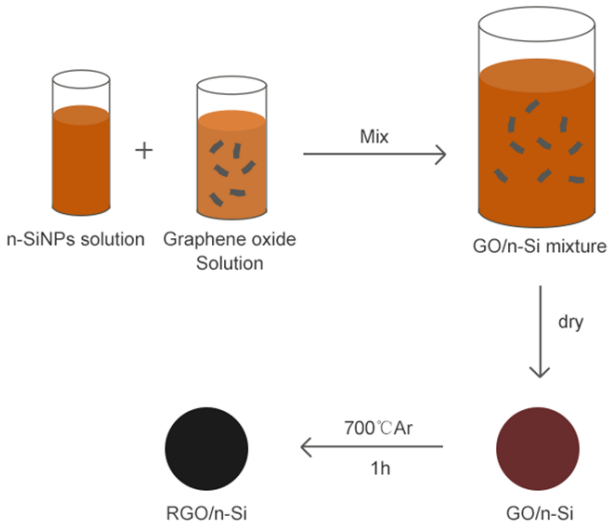

Figure 1. Schematic of the fabrication of RGO/n-Si composite

The structure of RGO/Si composite was displayed by SEM images. As shown in Figure 2a-d, the plicated sheets were RGO and granulated spheres were n-Si nanoparticles, which can be seen clearly. The n-Si nanoparticles were completely encapsulated by RGO, forming silicon nanoparticles coated with 3D graphene structure. It was widely believed that n-Si nanoparticles exposed to the surface of composite will react with the electrolyte, leading to the further consumption of electrolyte and anode composite along with the formation of unstable SEI film, and thus the damping of cyclic performance. Accordingly, the thermal reduced graphene in as-synthesized RGO/Si composite in the present work acted as an elastic skeleton which can prevent n-Si nanoparticles from exposing to electrolyte and buffer the deformation stresses.

As is shown in figure 2e, the n-Si nanoparticles are spherical which are more easily to disperse in the graphene skeleton and release the volume deformation stresses during Li^+ insertion/extraction than blocky n-Si nanoparticles. Figure 2f shows the TEM diffraction image of n-Si nanoparticles, indicating that the n-Si nanoparticles are polycrystal. Compared with monocrystalline Si nanoparticles, polycrystalline Si nanoparticles adapt more easily to the volume changes during Li+ insertion, which is ascribed to the uniform strains of polycrystalline Si nanoparticles.

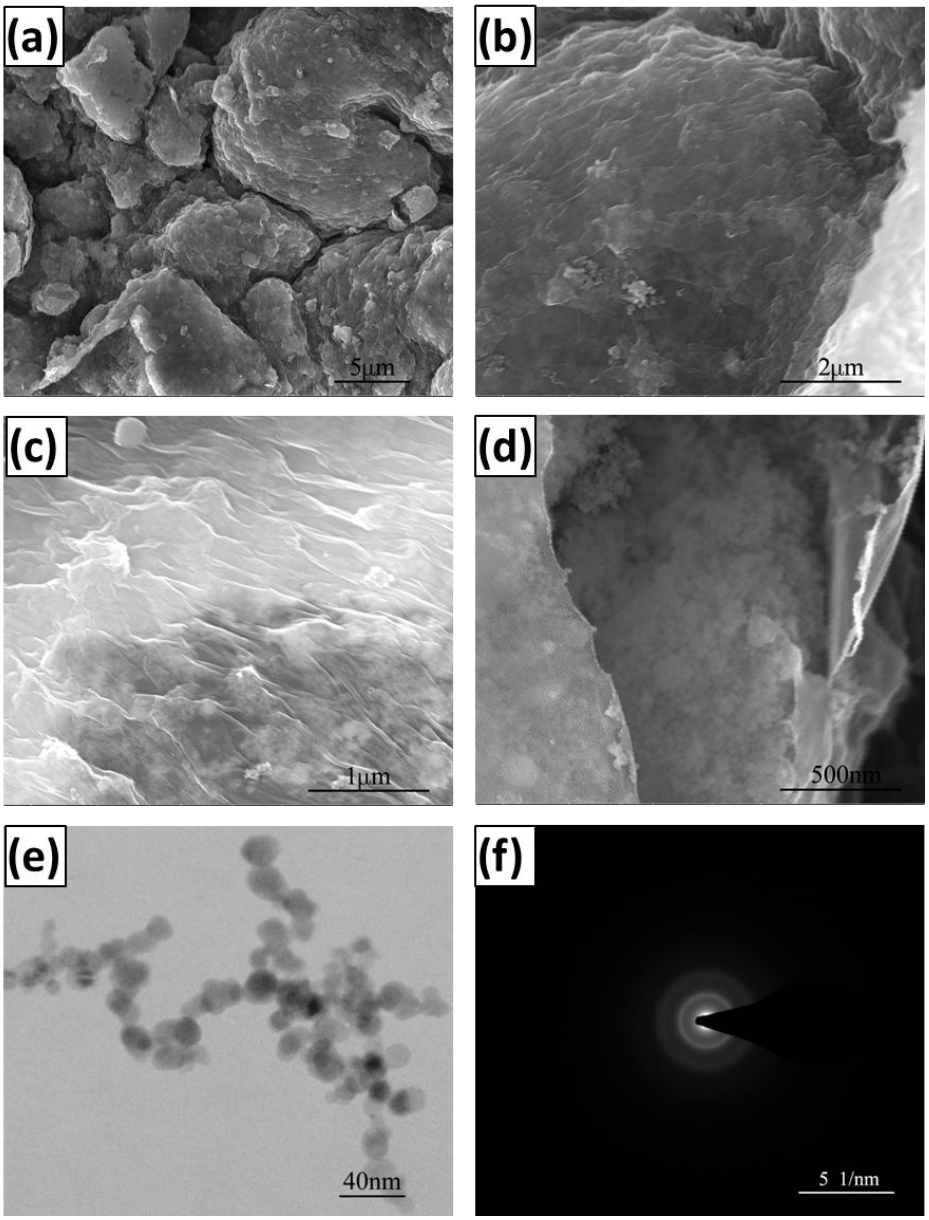

Figure 2. (a–d) SEM images of RGO/n-Si composite produced by thermal reduced at 700 ℃ under Ar; (e) TEM images of P doped Si nanoparticles though a plasma system; (f) TEM diffraction of P doping Si nanoparticles.

Figure 3a shows the XRD images of Si nanoparticles and RGO/n-Si composite, No obvious graphene diffraction peaks were observed in the XRD pattern, which indicate that the thermal reduced graphene is amorphous.

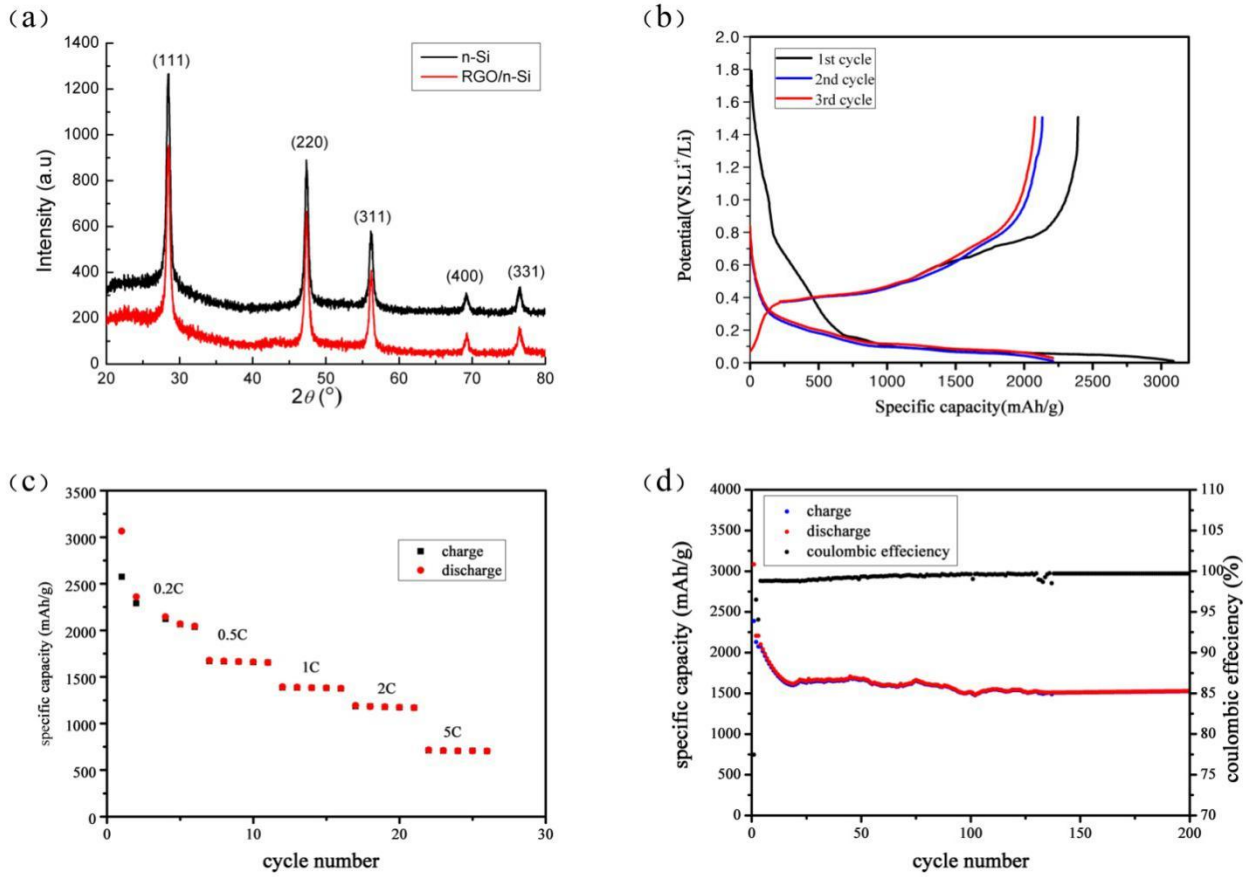

Figure 3. (a) XRD patterns of n-Si nanoparticles and n-Si nanoparticles coating with RGO; (b) galvanostatic dischargecharge profiles at C/5; (c) Ratecapability at the current rate of 0.2 C, 0.5 C, 1 C, 2 C and 5 C; (d) Cycling performance of Si/graphene composite at the current rate of 0.2 C.

To investigate the electrochemical performance of RGO/n-Si composite, 2025 coin half cells were fabricated with the RGO/n-Si composite on the Cu substrate as cathode and Li metal as the counter electrode. Figure 3b shows galvanostatic discharge/charge curves of RGO/n-Si composite with *vs*. Li/Li^+ in the potential range 0.01–1.5 V for the first three cycle at the current rate of C/5. A C-rate is a measure of the rate at which a battery is discharged relative to its maximum capacity. A 1 C rate means that the discharge current will discharge the entire battery in 1 hour[3]. The charge capacity is defined as the total charge inserted per unit mass of the materials during Li^+ insertion, whereas the discharge capacity is total discharge per unit mass of the materials during Li^+ extraction. [23] The first discharge and charge of RGO/n-Si composite was 3084mAh/g and 2388mAh/g, respectively. The first cycle coulombic efficiency (CE) was 77.5%. Usually, the intial coulombic efficiency of silicon-based anodes are below 80% due to the reactions with electrolytes and the formation of a SEI film on surface of the RGO/n-Si composite[24]. Which may be as a result of the high surface area of the graphene and the small amount of uncovered silicon nanoparticles. This may be solved through an artificial SEI layer by chemical modification[25,26]. However, in the second and third cycles, the coulombic

efficiency exceeds 94%, and the discharge capacities in the second and third cycles are both 2206 mAh/g.

Figure 3c shows the rate performance of RGO/n-Si composite. The discharge specific capacity of RGO/n-Si composite is 2036, 1654, 1280, 1168, and 705 mAh/g at the current rate of 0.2 C, 0.5 C, 1 C, 2 C, and 5 C, respectively. It can be obviously seen that the RGO/n-Si composite exhibit a good rate capability and maintains a high cyclic stability except the first 5 cycle at current rate of 0.2 C, which suggest the using of graphene and P doping silicon nanoparticles can reduce resistance for the interfacial electrochemical reaction and provide high way for Li^+ insertion and extraction.

Figure 3d shows the cyclic performance and coulumbic efficiency of the RGO/n-Si composite at the current rate of C/5 for 200 cycles. The specific capacity of the composite gradually decay at the first 25 cycle due to the SEI formation on the surface of RGO/n-Si and the reaction with electrolyte which will consume anode materials. In addition, the composite suggested an extremely stable cycle performance with specific capacity remaining at 1529 mAh/g for over 200 cycles which is three times higher than the commercial graphite anode materials (372 mAh/g) and nearly 100% coulombic efficiency in the subsequent cycles which attribute to the stable structure and good electrical conductivity of RGO/Si composite. That demonstrated the thermal reduced graphene worked as an elastic network which can envelop the Si nanoparticles for preventing exposure to electrolyte, buffering the deformation stresses and provide a pathway for Li^+ transport. Besides, silicon nanoparticles doping with P can also improve the electronic conductivity which contribute to the Li^+ insertion and extraction. Obviously, all the above results indicate that this structure of RGO/n-Si composite play a critical role in improving the specific capacity and cyclic stability of anode materials.

4. CONCLUSION

In summary, we have reported a approach for the synthesis of thermal reduced graphene oxide coated n-Si nanoparticles by a plasma system and CVD. It was found that the lithium-storage performance of RGO/n-Si composite material was dramatically improved, such as highly reversible lithium-storage capacity, prominent cyclic stability, and good rate capability. It has been demonstrated that the use of graphene as skeleton to encapsulate Si nanoparticles and TMP to dope Si nanoparticles are effective methods to improve the electrochemical performance of Silicon-based nanocomposite anode materials.

ACKNOWLEDGEMENTS

This work is supported by the National Basic Research Program of China (Grant No. 2012CB619302), the Science and Technology Bureau of Wuhan City (No. 2014010101010003), t Key Laboratory of infrared imaging materials and detectors, Shanghai Institute of Technical Physics, Chinese Academy of Sciences (Grant No. IIMDKFJJ-15-07), the National Natural Science Foundation of China (Grant No. 11574166), and the Director Fund of WNLO.

References

1. D. Aurbach, Z. Lu, A. Schechter, Y. Gofer, H. Gizbar, R. Turgeman, Y. Cohen, M. Moshkovich and E. Levil, *Nature*., 407 (2000) 724.
2. D. Bruce, G. Peter, B. Scrosati and J.M. Tarascon, *Angewandte Chemie International Edition*., 47 (2008) 2930.
3. Dunn Bruce, H. Kamath and J.M. Tarascon, *Science*., 334 (2011) 928.
4. J.M. Tarascon and M. Armand, *Nature*., 414 (2001) 359.
5. A. Michel and J.M. Tarascon, *Nature*., 451 (2008) 652.
6. B. Wang, X.L. Li, T.F. Qiu, B. Luo, J. Ning, J. Li, X.F. Zhang, M.H. Liang, and L.J. Zhi, *ACS Nano*., 7 (2013) 45.
7. A. Magasinski, P. Dixon, B. Hertzberg, A. Kvit, J. Ayala and G. Yushin, *Nature Materials*., 9 (2010) 8.
8. C.K. Chan, H.L. Peng, G. Liu, K. McIlwrath, X.F. Zhang, R.A. Huggins and Y. Cui, *Nature nanotechnology*., 3 (2008) 31.
9. M. Yoshioa, H.Y. Wang, K. Fukudac, T. Umenoc, N. Dimova and Z. Ogumib, *Journal of The Electrochemical Society*., 149 (2002) A1598.
10. Y.S. Hu, R.D. Cakan, M.M. Titirici, J.O. Müller Dr, R. Schlögl, M. Antonietti and J.Maier, *Angewandte Chemie International Edition*., 47 (2008) 1645.
11. S.D. Beattie, D. Larcher, M. Morcrette, B. Simonan and J.M. Tarascon, *J. Electrochem. Soc*., 155 (2008) A158.
12. A.I. Hochbaum, R.K. Chen, R.D. Delgado, W.J. Liang, E.C. Garnett, M. Najarian, A. Majumdar, and P.D. Yang, *Nature*., 451 (2008) 163.
13. S.B. Fagan, R.J. Baierle, R. Mota, A.J. da Silva and A. FazzioPhys, *Physical Review B*., 61 (2000) 9994.
14. S.Y. Jeong, J.Y. Kim, H.D. Yang, B.N. Yoon, S.H. Choi, H.K. Kang, C.W. Yang and Y.H. Lee, *Advanced Materials*., 15 (2003) 1172.
15. M.S. Arnold, A.A. Green, J.F. Hulvat, S.I. Stupp and M.C. Hersam, *Nature nanotechnology*., 1 (2006) 60.
16. M. Holzapfel, H. Buqa, F. Krumeich, P. Novák, F.M. Petrat and C. Veit, *Electrochemical Solid-State Letters*., 8 (2005) A516.
17. H. Jung, M. Park, S.H. Han, H. Lim, and S.K. Joo, *Solid State Communications*., 6030 (2003) 387.
18. L.F. Cui, Y. Yang, C. M. Hsu and Y. Cui, *Nano Letters*., 9 (2009) 3370.
19. J.K. Lee, K.B. Smith, C.M. Hayner and H.H. Kung, *Chemical Communications*., 46 (2010) 2025.
20. D.F. Wang, F.L. Li, G. X. Ping, D. Chen, M.Q. Fan, L.S. Qin, L.Q. Bai, G.L. Tian, C. Lu and K.Y. Shu, *Int. J. Electrochem. Sci*., 8 (2013) 9618.
21. C.J. Fu, C.L. Song, L.L. Liu, W.L. Zhao and X.D. Xie, *Int. J. Electrochem. Sci*., 11 (2016) 154.
22. T. Chen, B.Q. Zeng, J.L. Liu, J.H. Dong, X.Q. Liu, Z. Wu, X.Z. Yang and Z.M. Li, *Journal of Physics*., 188 (2009) 1.
23. J. Zhu, C. Gladden, N. Liu, Y. Cui and X. Zhang, *Physical Chemistry Chemical Physics*., 15 (2013) 440.
24. P. Verma, P. Maire and P. Novák, *Electrochim. Acta*., 55 (2010) 6332.
25. Q.M. Pan, H.B. Wang and Y.H. Jiang, *Electrochem. Commun*., 9 (2007)754.
26. Y.T. Lee, C.S. Yoon and Y.K. Sun, *J. Power Sources*., 139 (2005) 230–234.